END FORMING OF THIN-WALLED TUBES USING A DIE

Gouveia B. P. P.
IST, DEM, Av. Rovisco Pais, 1049-001 Lisboa, Portugal, e-mail: bgouveia@ist.utl.pt.
Alves M. L.
Instituto Politécnico de Leiria, Departamento de Engenharia Mecânica, Morro do Lena, 2400 Leiria, Portugal, e-mail: dinamrsa@estg.ipleiria.pt
Rosa P. A. R.
IST, DEM, Av. Rovisco Pais, 1049-001 Lisboa, Portugal, e-mail: pedro.rosa@ist.utl.pt.
Rodrigues J. M. C.
IST, DEM, Av. Rovisco Pais, 1049-001 Lisboa, Portugal, e-mail: jrodrigues@ist.utl.pt.
Martins P. A. F.
IST, DEM, Av. Rovisco Pais, 1049-001 Lisboa, Portugal, e-mail: pmartins@ist.utl.pt.

Abstract: *The term 'end forming of tubes' usually refers to a wide variety of shapes and profiles such as expansions, reductions, inversions, flares, flanges and tapers that can be obtained by means of single or multiple metal forming processes.*
Basic design rules for the end forming of thin-walled tubes using a die are mainly derived from the accumulated experience of both manufacturers of tubular parts and suppliers of machine-tools. Very few systematic studies have been done, as far as authors are aware, on the influence of process parameters on the formability limits induced by ductile fracture, wrinkling and local buckling. These topics are crucial for a wider comprehension of the mechanics of the process and for accomplishing an adequate characterization of the different modes of deformation (i.e. for successfully predicting the geometrical profiles found in daily practice).
The research work supporting this paper was based on a comprehensive numerical and experimental investigation on the expansion, reduction and nosing of thin-walled tubes using a die with the purpose of complementing some of the above mentioned gaps of knowledge.
The theoretical investigation was accomplished by the utilisation of virtual prototyping modelling techniques based on the finite element method and combines axisymmetric and three-dimensional simulations in order to successfully model the full geometrical details of the tube and tooling and to take into account the non-symmetric characteristics of certain modes of deformation that are induced by wrinkling, buckling and fracture. The experimental work on industrial Al6060 Aluminium alloy tubes under laboratory-controlled conditions was mainly utilized for supporting and validating the theoretical investigation.
Keywords: *End forming of tubes, Finite element method, Experimentation.*

1. INTRODUCTION

The expansion, reduction and nosing of tubes using a die is usually accomplished by forcing a tapered, dedicated punch (or die) into the tube end, and then retracting the punch (or die) back off after achieving the desired shape (please refer to Figure 1).

In general terms it can be stated that the expansion punch (Figure 1(a)) is dedicated to an outside radius r_p and a required length of expansion while the reduction die (Figure 1(b)) is dedicated to an inside radius r_d and a required length of reduction. The lengths of expansion and reduction are a function of the angle of inclination α and the design of each tool is limited to the specific initial reference radius r_0 of the tube. Each nosing die (Figure 1(c)) is dedicated to a specific nosing contour (e.g. a specific radius r_d in case of the hemispherical shaped dies) and its design is limited to the reference radius r_0 of the tube. l_{gap} refers to the initial gap height.

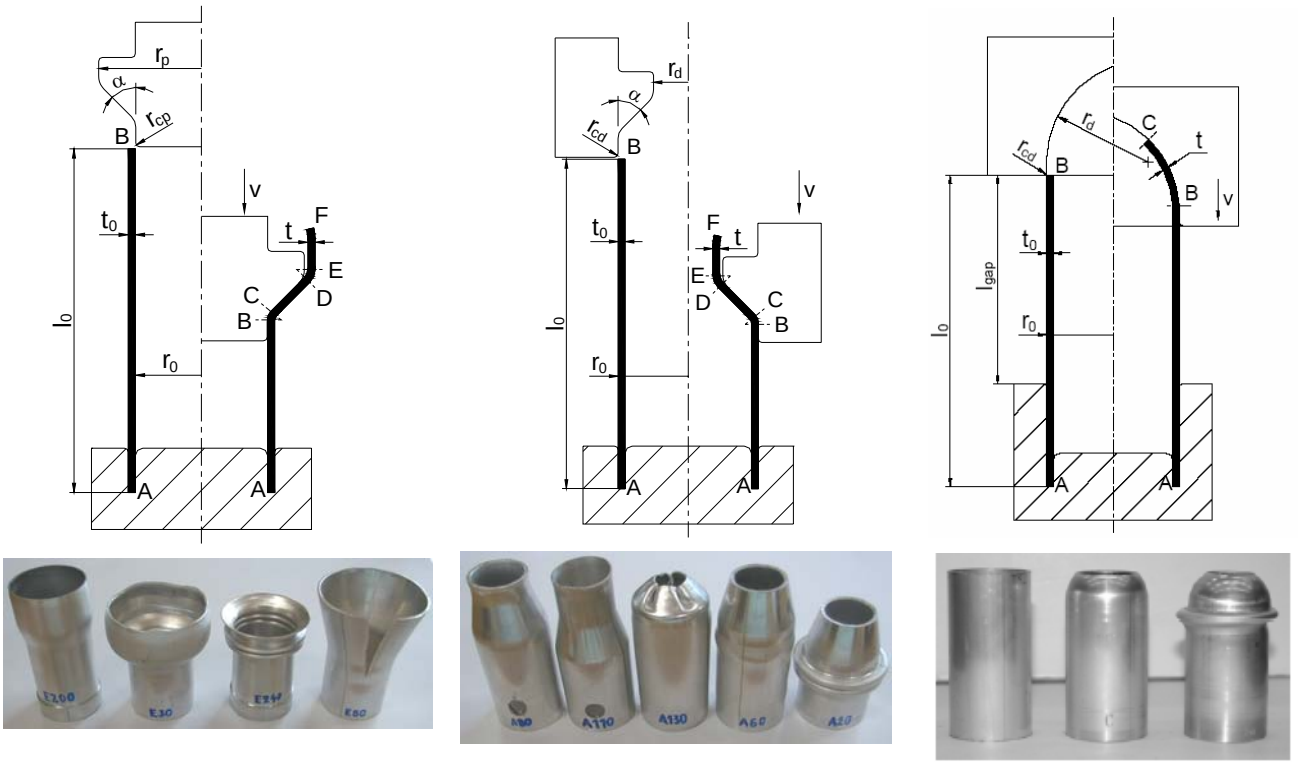

(a) (b) (c)

Figure 1. Schematic representation of the expansion (a), reduction (b) and nosing (c) of thin-walled tubes using a die, with some experimental parts showing typical modes of deformation that may occur.

All these three end forming processes comprise three different plastic deformation mechanisms; bending/unbending, stretching (or compression) along the circumferential direction θ and friction.

In the expansion and reduction of tubes bending takes place at point B, where the tube first contacts the punch (or die), while unbending takes place at point D, where the tube leaves contact with the punch (or die). Point E fixes the beginning of the free deformed region of the tube that spans from E to the leading edge F. The free deformed region of the tube undergoes near-rigid body motion. Stretching/compression develops while the tube gradually deforms over the punch (or against the die) – refer to CD in Figure 1 - top. The influence of friction predominantly occurs between points B and D

although, some minor restraint, is also likely to take place at the entrance of the punch (or die) – refer to the cylindrical surface ahead of point B.

In case of tube nosing bending takes place at point B, where the tube first contacts the die, compression develops as the tube gradually deforms against the die – refer to BC in Figure 1(c), and the influence of friction predominantly occurs between points B and C although, some minor restraint, is also likely to take place at the entrance of the die – refer to the small cylindrical guidance surface adjacent to point B.

2. EXPERIMENTAL BACKGROUND

2.1. Mechanical, tribological and formability conditions

The material employed in the experimental tests was an Al6060 aluminium alloy (natural aged). The stress-strain curve was obtained by means of tensile and compression tests carried out at room temperature[1] (please refer to Figure 2),

$$\overline{\sigma} = 298.3\overline{\varepsilon}^{0.0857} \text{ MPa} \quad (1)$$

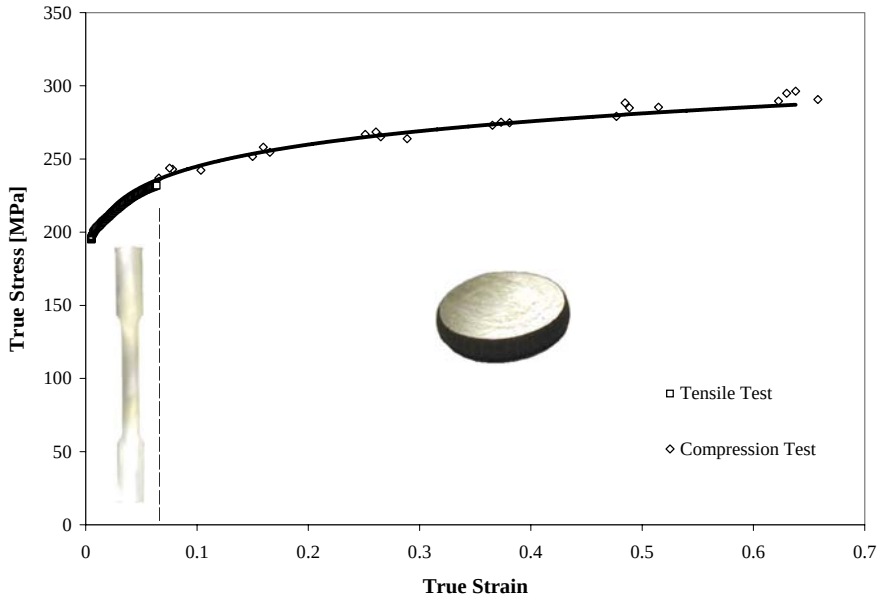

Figure 2. Stress-strain curve of the Al6060 aluminium alloy (natural aged) obtained by tensile and compression tests.

The tribological conditions at the contact interface between the tube and the die were estimated by means of ring compression tests on ring test samples (6:3:2 proportions) prepared according to the lubrication procedure utilized in the forming process (MoS_2 based lubricant). Interface friction was characterized by means of the law of constant friction, $\tau = mk$ and the friction factor m was found to be equal to 0.11 for MoS2 based lubricant according to calibration curves determined by finite element simulation (further details can be found elsewhere[2,5]).

The experimental procedure utilized to characterize the formability of the Al6060 Aluminium alloy was based on the evaluation of fracture strains of cylindrical upset tests specimens ($h/d = 2.5$) as suggested by Gouveia et al.[3]. A critical value of damage of 0.42 was obtained for the normalized Cockcroft-Latham criterion. No lubricant was utilised during the tests.

2.2. Experimental procedure

The experiments on end forming of thin walled tubes were performed on tubular specimens with a reference radius $r_0 = 18$ mm (tube expansion) and $r_0 = 20$ mm (tube reduction and nosing), and two different values of the wall thickness, $t_0 = 1.0$ mm and 2.0 mm. The length of the specimens was $l_0 = 90$ mm for tube expansion and reduction tests and $l_0 = 80, 90$ and 120 mm for tube nosing tests. The experiments were performed at a displacement rate of 1.17 mm/s and, therefore, no dynamic effects in the deformation mechanics of the tubes were taken into account.

The experiments were planned in order to consider the main process parameters that rule expansion, reduction and nosing operations of thin-walled tubes using a die; (i) the ratios r_p / r_0 (for expansion), r_d / r_0 (for reduction and nosing), (ii) the ratio t_0 / r_0, (iii) the angle α of the conical surface of the punch/die (for expansion and reduction) and (iv) lubrication. The influence of anisotropy was not taken into account.

Punches and dies with different geometries were utilized to obtain the desired end-forms of the tubes.

Further experimental details of the present investigation can be found elsewhere [5,6].

In order to allow load recording during experiments, force was applied to the punch through one load cell based on traditional strain-gauge technology in a full Wheatstone bridge. Punch displacements were measured using a micro-pulse position transducer. A PC-based data logging system was used to record and store loads and displacements.

The critical plastic instability load P_{cr} for the occurrence of local buckling was determined by means of the axial compression of tubes between flat dies in accordance with the experimental procedure previously described by Rosa et al.[1]. Critical plastic instability loads $P_{cr} = 21.5$ kN and $P_{cr} = 46.8$ kN were respectively measured for tubular wall thicknesses $t_0 = 1.0$ and 2.0 mm.

3. THEORETICAL BACKGROUND

3.1. Finite element flow formulation

The numerical modelling of the tubes end forming operations was performed using the computational programs I-FORM2 (two dimensional) and I-FORM3 (three dimensional) developed at Instituto Superior Técnico. The programs perform a rigid-plastic/viscoplastic analysis of metal forming processes based on the finite element flow formulation.

The flow formulation based on the penalty function method is based on the minimization of the following variational statement (2),

$$\pi = \int_V \overline{\sigma}\,\dot{\overline{\varepsilon}}\, dV + \tfrac{1}{2} K \int_V \dot{\varepsilon}_v^2\, dV - \int_{S_T} T_i u_i\, dS + \int_{S_f} \left(\int_0^{|u_r|} \tau_f\, du_r \right) dS \qquad (2)$$

where, K is a large positive constant enforcing the incompressibility constraint and V is the control volume limited by the surfaces S_U and S_T, where velocity and traction are prescribed, respectively, and S_f is the contact friction interface. The numerical model of the interface friction was performed by means of the constant friction factor, $\tau = mk$, where friction is considered as a traction boundary condition, leading to a power consumption term due to friction, where u_r is the relative velocity and, τ_f is the friction shear stress between the tube and the tooling.

3.2. Modelling conditions

Finite element computer models were set-up in order to reproduce all the experimentally observed modes of deformation. The three-dimensional characteristics of the material flow associated with the majority of these modes of deformation, required discretization of the tubular specimens by means of eight-node hexahedral elements and definition of the punches and dies by the use of contact-friction linear triangular elements.

On account of rotational symmetry of some modes of deformation it was also possible to employ axisymmetrical numerical models based on the discretization of the initial cross section of the tubular specimens by means of four-node quadrilateral elements and on the description of the contour of the dies through the utilization of contact-friction linear elements.

Three dimensional models were calculated by I-FORM3 while axisymmetrical models made use of I-FORM2. In both cases, modelling was accomplished through a succession of displacement increments each of one corresponding to approximately 0.5% of the initial tube length.

Computer runs were performed with varying element numbers in the thickness direction of the tube in order to analyse the influence of mesh discretization in the overall quality of the numerical predictions and in the total CPU time. In case of three-dimensional finite element analysis a similar load-displacement trend was found to exist when employing two, three or four elements in the thickness direction. In what concerns CPU time the comparison between the three-dimensional CPU run times becomes meaningless when clocking less than 2 min for finishing a two-dimensional finite element simulation. The compromise between the quality of the results provided by three-dimensional finite element simulations and the overall CPU run time constrained the authors to employ 3D models with only three elements in the thickness direction.

In general terms, it can also be concluded that the two-dimensional prediction of the forming load is more accurate than the three-dimensional due to the fact that three-dimensional modelling requires up to an order of magnitude more elements than those employed in the investigation to achieve the same level of accuracy as two-dimensional. Because such an alternative would result in much slower CPU run times, this turns two-dimensional modelling into a preferred choice for the analysis of the axysimmetric modes of deformation of tube end - forming operations.

Even so, two examples of the importance of three-dimensional simulations will be given in next section; one is a tube expansion operation where the crack propagation along the axial direction of an axysimmetric tube model could only be achieved by means of a three-dimensional finite element strategy based on the physical separation of adjacent elements at the nodal points where ductile damage reached critical values, and the other is a tube reduction operation where the physical mechanism of wrinkling could not be properly addressed by axisymmetrical finite element modelling.

4. RESULTS AND DISCUSSION

The work on tube expansion confirmed the existence of three different modes of deformation (Figure 1(a)). For large ratios of r_p/r_0 and high values of the angle α, formability is limited by the occurrence of plastic instability while for larger lengths of expansion ($\alpha <<$) restrictions are normally set by ductile damage (fracture) in the regions that are highly stretched in the circumferential direction.

The work on tube reduction also revealed the existence of three different modes of deformation (Figure 1(b)). For small values of r_d/r_0 and small lengths of reduction formability is mainly limited by the development of plastic instability modes whilst for larger lengths of reduction restrictions are normally set by excessive thickening of the tube wall and by the occurrence of wrinkling at the conical wall of the tubes.

The work on tube nosing allowed the identification of two different modes of deformation (Figure 1(c)), with the unsuccessful tubular part being originated by a material flow mechanism

resulting from local buckling. The success of a tube nosing operation and the total amount of nosing is very much influenced by a set of process parameters related to the initial gap height (l_{gap}/r_0), contour of the die (r_d/r_0), thickness of the tube wall (r_0/t_0) and lubrication conditions at the contact interface between the tube and die.

In the expansion, reduction and nosing of tubes the energy is dissipated in two different ways; one by friction at the contact interface between the tooling and the tube, and the other by the plastic work done in deforming the tube. The importance of friction and lubrication in the overall formability of the processes is illustrated in Figure 3 where a successful tube reduction can easily be replaced by a non-successful mode of deformation simply by changing the lubrication regime.

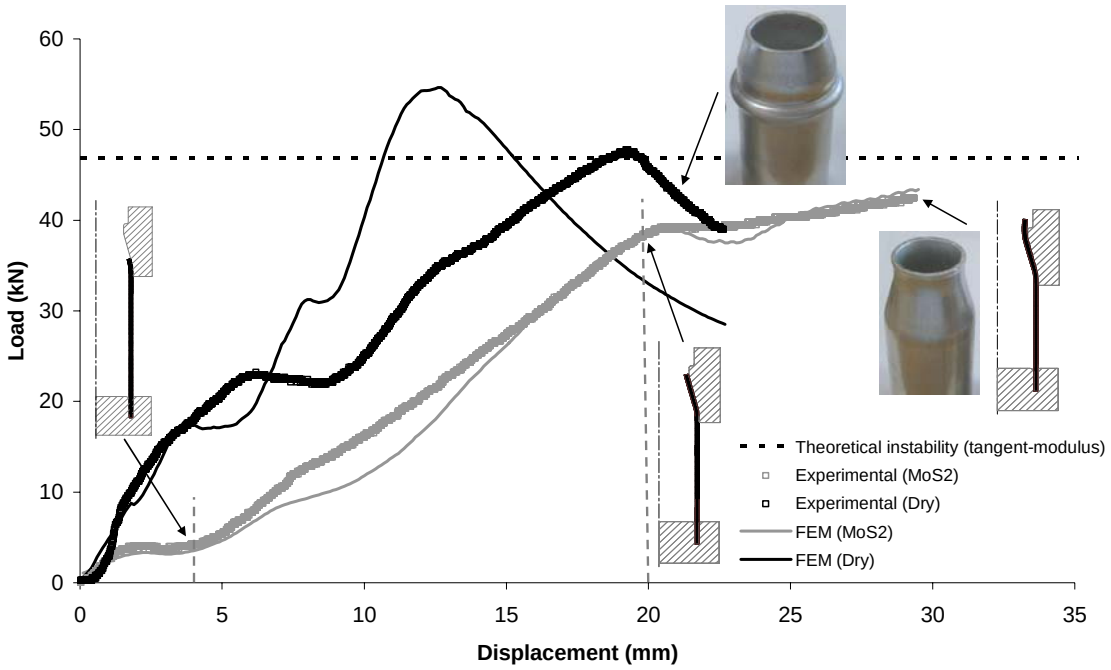

Figure 3. Theoretical and experimental evolution of the load-displacement curve under different lubricant conditions for the reduction of thin-walled tubes using a die ($t_0 = 2.0\,\text{mm}$, $r_d/r_0 = 0.75$ and $\alpha = 15^o$).

The examination of the predicted and experimental load-displacement curve for the tube reduction cases included in Figure 3 allow the identification of three different forming stages: (i) the initial axial compression stage after which the tube bends axially in order to match the conical surface of the die, (ii) the transient reduction stage when the leading edge of the tube starts to flow along the conical surface of the die and, as a consequence of progressive circumferential compression, the load grows moderately from a lowered level, and (iii) the final stage where steady-state reduction or local buckling stages occur dependent on the use of lubricant or not: in the lubricated case under analysis a successful mode of deformation is developed and steady-state conditions are reached after unbending of the leading edge of the tube at point D. The forming load, P_f, in steady-state conditions is approximately constant; in the non-lubricated case the tube develops an instability before his leading edge reaches the end of the die. This is due to a much higher rate of load grow owing to the increase of friction and to a peak value of the forming load above the critical instability load $P_f > P_{cr}$.

It is important to notice that the value of the forming load P_f must be regarded as a necessary, but not a sufficient, condition for the occurrence of local buckling in tube end forming operations. The tube

nosing operation with a small l_{gap} is an example of this. Figure 4 presents a comparison between the experimental and the finite element predicted evolution of the forming load as a function of the displacement of the upper-die for tube nosing using an hemispherical contour die of $r_d = 25\,\text{mm}$ and tubes with different initial gaps, l_{gap}. Numerical and experimental curves compare well and insets show pictures of deformed specimens and details of finite element numerical models at various stages of deformation.

Two different forming stages can be identified for all cases; an initial stage where the evolution of the load vs. displacement is smooth and a subsequent stage in which the load grows moderately from a lowered level. The pattern of the initial stage is similar to that commonly observed in the reduction of thin walled tubes with small reduction-of-area ratios while the pattern of the second stage is the consequence of increasing circumferential compression as the leading edge of the tube end is deformed by the upper die.

The cases with a higher initial gap height disclose a third forming stage corresponding to local buckling and to the development of an unsuccessful mode of deformation. This is found to occur when the peak value of the forming load reaches the critical instability load, P_{cr}.

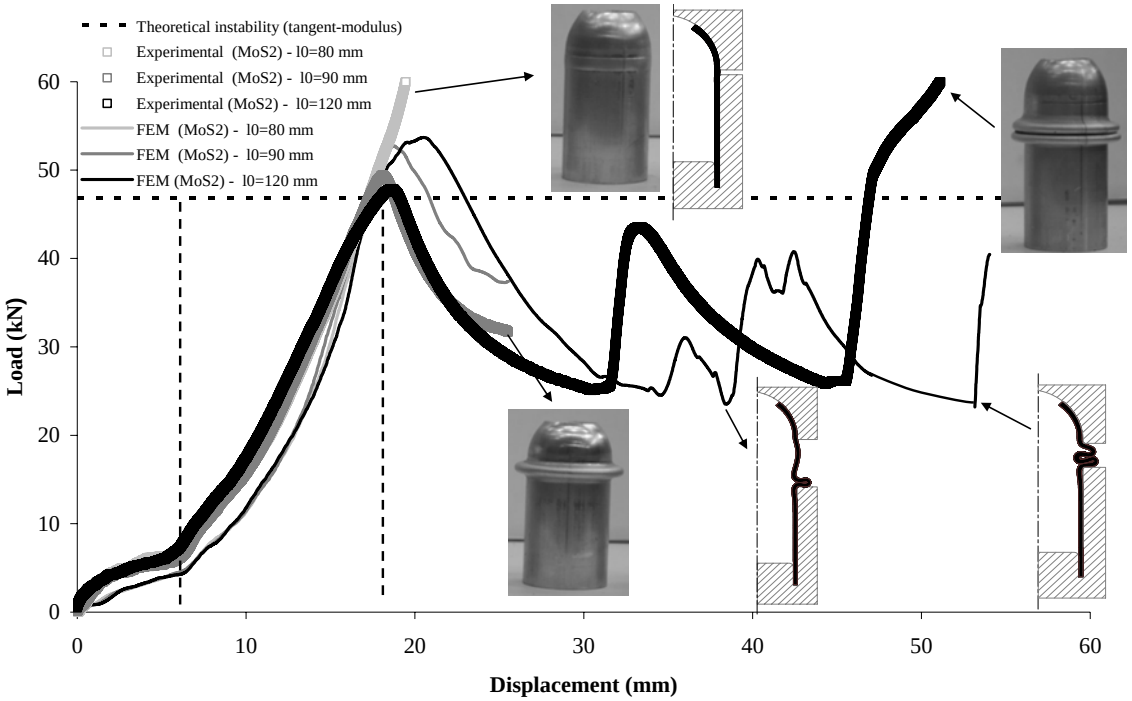

Figure 4. Theoretical and experimental evolution of the load-displacement curve for three tube nosing operations ($t_0 = 2.0\,\text{mm}$, $r_d / r_0 = 1.25$ and lubricated) with different initial gap heights $l_{gap} = 27, 37 \text{ and } 67\,\text{mm}$.

Under these circumstances, the value of the forming load P_f must be regarded as a necessary, but not a sufficient, condition for the occurrence of local buckling during tube nosing operations because the forming load, in the case with $l_{gap} = 27\,\text{mm}$, is found to growth high above the critical instability load without promoting the development of an unsuccessful mode of deformation. In fact, the initial gap height also plays an important role in the overall success of the tube nosing operation because it controls the amount of free space for the tube to buckle. This last observation allows us to conclude

that the total amount of nosing can significantly be changed by setting the initial gap height and properly choosing the process parameters that will allow the forming load to go high above the instability limit.

(a) (b) (c)

Figure 5. Reduction of thin-walled tubes using a die ($r_d / r_0 = 0.75$ and $\alpha = 15^o$). (a) Experimental part showing the wrinkled upper part ($t_0 = 1.0$ mm), (b) Top view of the part correspondent to (a), (c) Experimental part ($t_0 = 2.0$ mm)

The analysis of tube reduction operations revealed the influence of the wall thickness in formability limit. Figure 5 (a) and (c) show experimental parts obtained by tube reduction ($r_d / r_0 = 0.75$ and $\alpha = 15^o$) with wall thicknesses of 1.0 mm and 2.0 mm, respectively. In both operations no local bulking occurred and the tube reached the free deformed region at exit of the die. But a non-successful mode of deformation was obtained for the thinnest wall, $t_0 = 1.0$ mm, due to the occurrence of wrinkling at the upper region of the tube (Figure 5 (a) and (b)) caused by high compressive values of the circumferential stress, σ_θ, acting at the unsupported conical wall of the tubes. Because reduction induces compressive stresses at conical section of the tube, the minimum r_d / r_0 that can be taken in a single operation is limited not only by the axial collapse of the tube but also by the occurrence of wrinkles. As observed, for small values of t_0 / r_0 restrictions are generally set by excessive thickening of the tube wall and, therefore, by the occurrence of wrinkling. This conclusion is also valid for tube nosing operations.

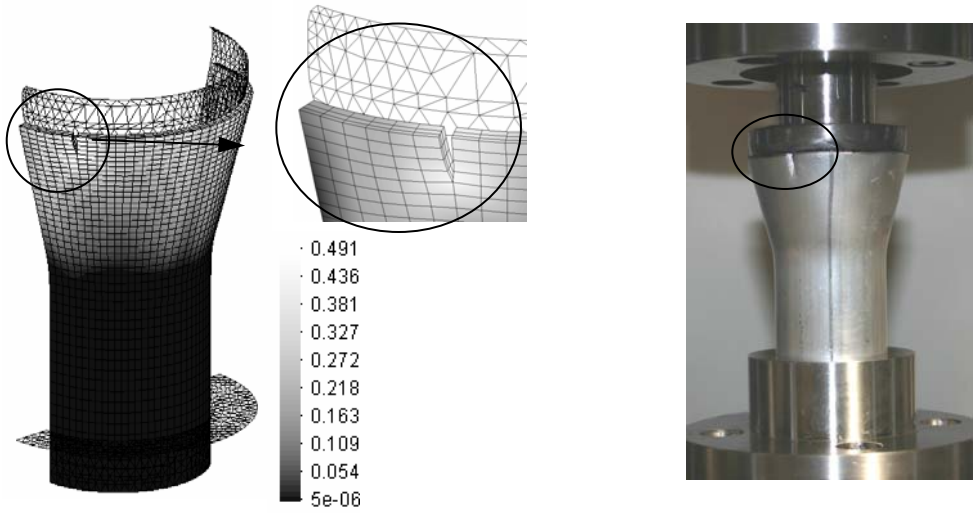

Figure 6. Theoretical distribution of the normalized Cockcroft-Latham ductile damage criterion during the expansion of a thin-walled tube ($t_0 = 2.0$ mm, $r_p / r_0 = 1.76$ and $\alpha = 15^o$) with the correspondent experimental part showing fracture.

Figure 6 presents theoretical distribution of ductile damage according to the Cockcroft-Latham, normalized criterion for the expansion of tubes with $t_0 = 2.0\,\text{mm}$, $r_p / r_0 = 1.76$ and $\alpha = 15^\circ$ obtained by means of a three-dimensional finite elements analysis. The theoretical distribution of damage, obtained shortly after the beginning of fracture, successfully estimates its peak value to occur at the tip of the crack located at the upper end of the tube according to the critical value of 0.42 (please refer to section 2.1) and to the experimental result (right side of Figure 6). It is worth mentioning that a correct reproduction of the experimental decrease of the forming load after reaching the onset of cracking can only be achieved by means of a three-dimensional finite element strategy based on the physical separation of adjacent elements at the nodal points where ductile damage reached critical values.

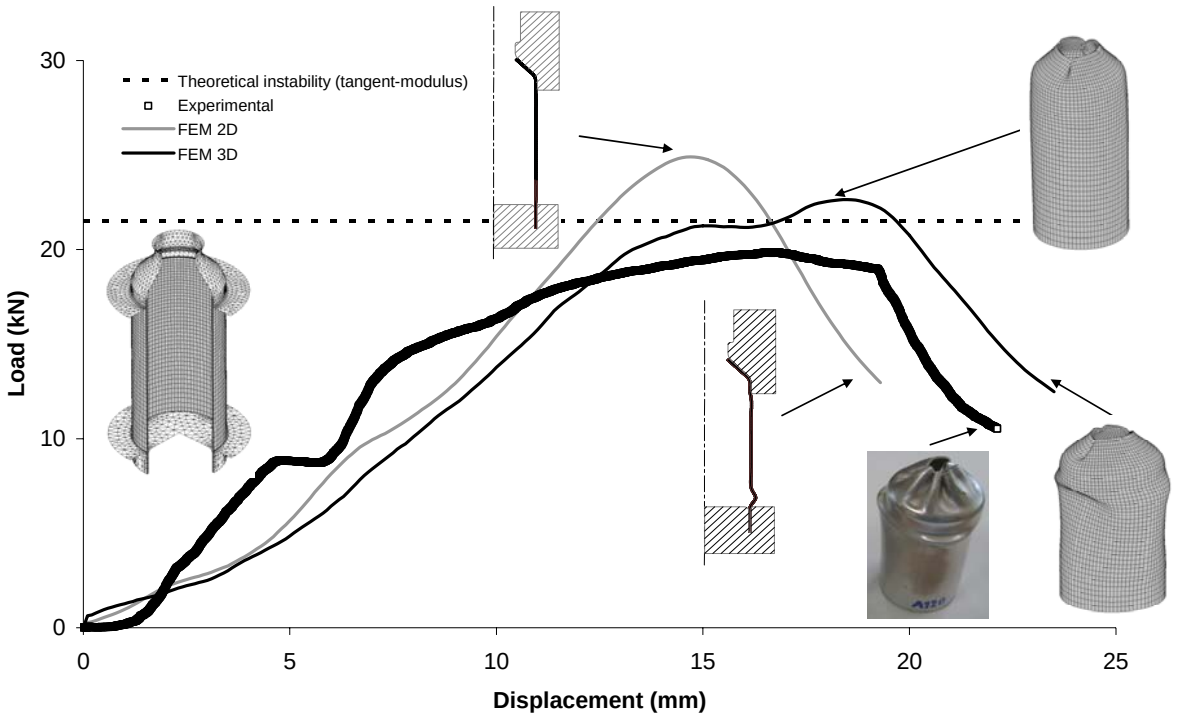

Figure 7. Theoretical and experimental evolution of the load-displacement curve for the reduction of thin-walled tubes ($r_d / r_0 = 0.5$, $\alpha = 45^\circ$, $t_0 = 1.0$ mm, lubricated)

Figure 7 presents the theoretical and experimental evolution of the forming load vs displacement for the reduction of tubes with $t_0 = 1.0\,\text{mm}$, $r_d / r_0 = 0.5$ and $\alpha = 45^\circ$. The insets show tubular specimens and details of the finite element predicted shapes at various stages of deformation add further refinements to the conventional wrinkling collapse mechanism. Besides the well known effect of the compressive circumferential stress, $\sigma_\theta = \sigma_3$, acting at the unsupported conical region of the tubes, it is also possible to confirm the effect that the excessive thickening of the upper tube wall has in creating an extra resistance to deformation that will be responsible for building up a peak forming load within the range of instability ($P_f \cong P_{cr}$). This is the reason why tubular specimens usually buckle shortly after the occurrence of the first wrinkles. The essence of the proposed wrinkling collapse mechanism is corroborated by the experimental and finite element predicted shapes in Figure 7.

Under these circumstances, it is now possible to understand the reason why the two-dimensional expected evolution of the forming load does not match with the experimental data plotted in Figure 7. In fact, the physical mechanism of wrinkling is dictated by three-dimensional material flow and, therefore, can not be properly addressed by axisymmetrical finite element modelling. Two-dimensional

models are only capable of addressing the excessive thickening of the tube wall and the correspondent increase of the forming load beyond the onset of instability. In other words, the axisymmetric finite element models simply predict the occurrence of local buckling instead of envisaging the wrinkles that will subsequently induce local buckling.

5. CONCLUSIONS

Design rules and process parameters for the end forming of thin-walled tubes using a die must be properly established/chosen so that material deformation does not approach formability limits due to ductile fracture, local buckling and wrinkling. Tube wall thickness and lubrication play a key role in obtaining a successful mode of deformation.

Admissible values of the major process parameters are usually bounded by values that give rise to buckling and values that stimulate the occurrence of cracking (expansion) or wrinkling (reduction and nosing).

Some cases of tube nosing are capable of withstanding forming loads high above the value of the critical instability load without developing local buckling.

The utilisation of ductile fracture criteria and/or forming limit diagrams in conjunction with the numerical modelling of the process is able to provide an adequate understanding of the incidence of fracture.

Results demonstrate that finite elements can be successfully employed for evaluating the overall performance of tooling and raw material as well as to debug undesirable manufacturing occurrences. This opens the possibility of reducing and eliminating expensive and time-consuming industrial try-outs when designing other sophisticated tube end shapes.

6. REFERENCES

1. ROSA, P. A. R., RODRIGUES, J. M. C. and MARTINS, P. A. F., External Inversion of Thin-Walled Tubes Using a Die: Experimental and Theoretical Investigation, Int. J. Mach. Tools & Manuf., 43, 787, 2003.
2. ROSA, P. A. R., RODRIGUES, J. M. C. and MARTINS, P. A. F., Internal Inversion of Thin-Walled Tubes Using a Die: Experimental and Theoretical Investigation, Int. J. Mach. Tools & Manuf., 44, 775, 2004.
3. GOUVEIA, B. P. P. A., RODRIGUES, J. M. C. and MARTINS, P. A. F., Fracture prediction in bulk metal forming, Int. J. Mech. Sci., 38, 361, 1996.
4. ATKINS, A. G. and MAI, Y.-W., Elastic and plastic fracture, Wiley, New York, 1985.
5. ALMEIDA, B. P. P., ALVES, M.L., ROSA, P.A.R., BRITO, A.G., MARTINS P.A.F., Expansion and reduction of thin-walled tubes using a die: Experimental and theoretical investigation, Int. J. Mach. Tools & Manuf., v. 46, 12-13, p. 1643-1652, October 2006.
6 ALVES M. L., GOUVEIA B. P. P., ROSA P. A. R. and MARTINS P. A. F., On the Analysis of the Expansion and Reduction of Thin-Walled Tubes Using a Die, J. Eng. Manufacture, accepted for publication, 2006.